

A probable pre-main sequence chemically peculiar star in the open cluster Stock 16

M. Netopil¹*, L. Fossati², E. Paunzen¹, K. Zwintz³, O. I. Pintado⁴ and S. Bagnulo⁵

¹*Department of Theoretical Physics and Astrophysics, Masaryk University, Kotlářská 2, 611 37 Brno, Czech Republic*

²*Argelander-Institut für Astronomie der Universität Bonn, Auf dem Hügel 71, 53121 Bonn, Germany*

³*Instituut voor Sterrenkunde, KU Leuven, Celestijnenlaan 200D, 3001 Leuven, Belgium*

⁴*Instituto Superior de Correlación Geológica, CONICET, Miguel Lillo 205, 4000 San Miguel de Tucumán, Argentina*

⁵*Armagh Observatory, College Hill, Armagh BT61 9DG, Northern Ireland, UK*

ABSTRACT

We used the Ultraviolet and Visual Echelle Spectrograph of the ESO-Very Large Telescope to obtain a high resolution and high signal-to-noise ratio spectrum of Stock 16-12, an early-type star which previous Δa photometric observations suggest being a chemically peculiar (CP) star. We used spectral synthesis to perform a detailed abundance analysis obtaining an effective temperature of 8400 ± 400 K, a surface gravity of 4.1 ± 0.4 , a microturbulence velocity of $3.4^{+0.7}_{-0.3}$ km s⁻¹, and a projected rotational velocity of 68 ± 4 km s⁻¹. We provide photometric and spectroscopic evidence showing the star is most likely a member of the young Stock 16 open cluster (age 3–8 Myr). The probable cluster membership, the star's position in the Hertzsprung-Russell diagram, and the found infrared excess strongly suggest the star is still in the pre-main-sequence (PMS) phase. We used PMS evolutionary tracks to determine the stellar mass, which ranges between 1.95 and 2.3 M_{\odot} , depending upon the adopted spectroscopic or photometric data results. Similarly, we obtained a stellar age ranging between 4 and 6 Myr, in agreement with that of the cluster. Because the star's chemical abundance pattern resembles well that known of main sequence CP metallic line (Am) stars, the object sets important constraints to the diffusion theory. Additional spectroscopic and spectropolarimetric data allowed us to conclude that the object is probably a single non-magnetic star.

Key words: stars: abundances – stars: chemically peculiar – stars: individual: Stock 16 12 – stars: pre-main-sequence – open clusters and associations: individual: Stock 16

1 INTRODUCTION

The classical metallic-line stars of the upper main sequence (often denoted as Am/Fm or CP1 stars), are A- to early F-type objects (Preston 1974). These stars, as such, were first described by Titus & Morgan (1940) using spectra of Hyades cluster members. In general, Am stars are characterized by overabundances of metallic elements heavier than iron, whereas calcium, scandium, carbon, nitrogen and oxygen are underabundant.

There are two different models based upon atomic diffusion to explain the Am phenomenon. Watson (1971) proposed that the separation of chemical elements occurred just below the hydrogen convection zone where calcium has a small radiative acceleration. This implies that on the main sequence (MS) a very small mass fraction has anomalous abundances. In the subgiant phase, the anomalies will be diluted due to the increased mixing. In the other model, proposed by Richer, Michaud & Turcotte (2000), the separation occurs much deeper in the stellar interior. Therefore, on the MS, a much larger mass fraction has anomalous abundances. As

a consequence, the chemical peculiarities remain for a longer time as the star evolves on the subgiant branch: the abundance anomalies remain visible till convection dominates.

The chemical separation resulting from atomic diffusion can affect both the surface and interior of pre-main sequence (PMS) stars (Vick et al. 2011) and the mass in the different convection zones and internal elemental concentrations can be already modified before a star arrives on the MS. The amplitude of the internal abundances depends on the stellar mass; equivalently, the age at which abundance anomalies appear at the stellar surface also depends on the stellar mass. In the presence of weak mass loss, and no turbulent mixing, rotation or magnetic fields, significant internal variations and surface anomalies can appear already after about 2 Myr in early A-type stars, and at about 20 Myr in cooler F-type stars. To constrain these models it is essential to know when the Am phenomenon first appears on the PMS, but a PMS Am star has not yet been found so far.

For another group among the chemically peculiar (CP) stars (the magnetic Bp/Ap objects), there were already efforts to identify representatives on the PMS. However, up to now only one possible candidate with weak Ap/Bp peculiari-

* E-mail: mnetopil@physics.muni.cz

ties (V380 Ori A) was detected (Folsom et al. 2012). Recently, Bailey, Landstreet & Bagnulo (2014) presented the time-dependent evolution of chemical abundances for (MS) cluster Bp stars. A similar approach for Am objects and the detection of a PMS prototype is important to provide further observational constraints to the diffusion theory and on the time-scale of the evolution of the chemical abundances of CP stars. In order to search for PMS CP stars, observations of open clusters are preferable because they contain samples of stars of well constrained age and homogeneous initial chemical composition, characteristics suited for the study of processes linked to stellar structure and evolution.

The paper is arranged as follows. In Section 2 we describe the open cluster and the target star. A detailed spectroscopic analysis of the target star is presented in Section 3. These results are essential to provide further constraints on the cluster membership and evolutionary stage (Section 4). In Section 5 we discuss the results, and Section 6 concludes the paper.

2 TARGET STAR AND HOST OPEN CLUSTER

The young open cluster Stock 16 is located in the H II region RCW 75, which furthermore appears to be part of the extended associations Cen OB1 and Cen R1 (Turner 1985). The first detailed investigation of the cluster was carried out by Fenkart et al. (1977) in the photographic *RGU* system, followed by the photoelectric *UBV* study by Turner (1985). Later on, Vázquez et al. (2005) presented a deep CCD multi-colour investigation and identified several PMS objects. Finally, Paunzen et al. (2005b) studied the cluster in the Δa photometric system as part of a survey to detect CP stars. All mentioned studies agree in the obtained cluster parameters. Using the individual results, we derived the average values $E(B - V) = 0.51 \pm 0.02$ mag for the reddening and 1910 ± 85 pc for the distance. Since the cluster's metallicity is not known, which strongly influences the distance determination, the uncertainty on the distance is very probably underestimated. We therefore adopt a more realistic value of about 10 per cent (~ 200 pc). In the literature (Turner 1985; Paunzen et al. 2005b; Vázquez et al. 2005) the cluster age is estimated to be between 3 and 8 Myr. Hence, at such a young age, cluster stars with spectral type A and later are most likely still in their PMS stage. Fig. 1 shows the dereddened colour-magnitude diagram (CMD) of the cluster.

Note that the cluster position given in SIMBAD and in the open cluster data base WEBDA¹ (Mermilliod & Paunzen 2003) disagrees by about 10 arcmin with the one used by all the aforementioned studies. Because of this offset, Santos-Silva & Gregorio-Hetem (2012) obtained for the cluster a rather low stellar density contrast to the background. However, this study derived values for the age and the distance similar to the ones of Stock 16 listed above, but a reddening lower by ~ 0.2 mag. Nevertheless, this provides a further proof of a young area, which probably exhibits strong differential reddening.

The OB association Cen OB1 was studied by Kalcheva & Georgiev (1994) based on Strömgren photometry for two dozen stars. They obtained a distance of ~ 2.3 kpc, an age of about 9 Myr, and a strong differential reddening in $E(B - V)$ between 0.3 and 1.1 mag, not uncommon for a dusty region. Corti & Orellana (2013) derived a somewhat larger distance of $\sim 2.6 \pm 0.5$ kpc, an average radial velocity of $v_r = -20.0$ km s⁻¹ and

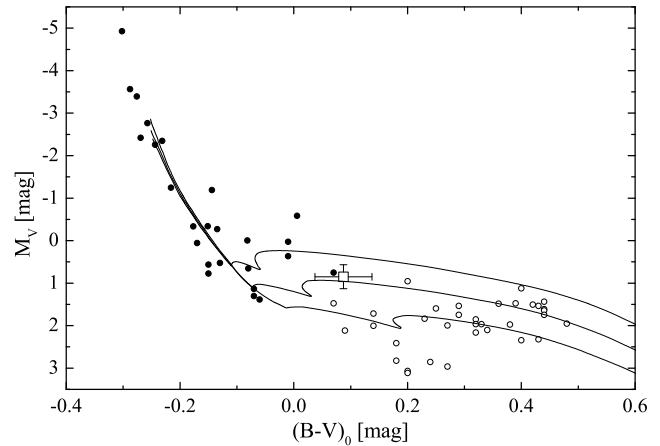


Figure 1. The CMD of Stock 16 based on member stars listed by Turner (1985) and Vázquez et al. (2005). Probable PMS objects identified by Vázquez et al. (2005) are indicated by open circles, while the target star Stock 16-12 is marked by an open square. Whenever applicable, the stars were individually dereddened as described in Section 4, otherwise the average $E(B - V) = 0.51$ mag was applied. The average cluster distance of 1910 pc was used to derive the absolute magnitudes. The isochrones for 3, 5, and 8 Myr by Bressan et al. (2012), which include the PMS phase, are shown as solid lines.

an average proper motion of $-4.78 \pm 0.10 / -0.93 \pm 0.10$ mas yr⁻¹. The latter is identical to the one listed by Zejda et al. (2012) for Stock 16 ($-5.0 \pm 0.4 / -0.9 \pm 0.4$ mas yr⁻¹). A much closer distance of 1.8 ± 0.4 kpc was instead found by Kalcheva, Golev & Moran (2014). They attribute the large difference to an overestimation of the absolute magnitude when using spectral types and standard relations.

Hence, as already pointed out by Turner (1985), there is a strong evidence that Stock 16 is a member of an extended structure, which includes at least one further confirmed young open cluster (NGC 4755; Corti & Orellana 2013) with parameters nearly identical to that of Stock 16.

The photometric study by Paunzen et al. (2005b) detected a probable CP star in the area of Stock 16 (Stock 16-12: $V \sim 13.4$ mag, J2000 RA 13:18:51, Dec. $-62:29:22$) due to a positive peculiarity index ($\Delta a = +24$ mmag). Such a value is in general indicative of characteristics typical of magnetic CP stars (Paunzen, Stütz & Maitzen 2005a). Later, the star was classified as A2 Si with strong metals by Paunzen et al. (2011) based on a low-resolution spectrum (2 \AA pixel^{-1}). The problems arising in the classification of the various peculiar groups are extensively discussed by Jaschek & Jaschek (1974), and one also can not exclude a bias in the classification process due to the measured Δa . However, the noticeable strong metals are already a hint for a later type star and hence a possible nature as metallic-line (Am) star as found in Section 3. Only some representatives of this group show positive Δa values, but Paunzen et al. (2005b) used the apparent and not intrinsic colours for the diagnostic Δa diagram. The somewhat lower reddening of Stock 16-12 compared to the cluster's mean (see discussion in Section 4) shifts the star to redder colours in the diagram, resulting in an insignificant Δa value.

We obtained an additional spectrum of this star with the 2.15m telescope at the Complejo Astronómico el Leoncito (CASLEO) on 2012 May 11 using the same configuration as given by Paunzen et al. (2011), except for a small shift in the blaze angle.

¹ <http://webda.physics.muni.cz/>

With the new information provided in the present paper, we would classify Stock 16-12 as kA2 hA3 mA7 based on the Ca II K, hydrogen, and metallic lines. There are no noticeable differences between the two available low resolution spectra, though both exhibit a low signal-to-noise ratio (S/N) of ~ 25 . We therefore decided to acquire an additional higher quality spectrum for a detailed analysis, which is presented in Section 3.

3 SPECTROSCOPIC ANALYSIS

We obtained one spectrum of Stock 16-12 on 2013 May 20 with the Ultraviolet and Visual Echelle Spectrograph (UVES) of the ESO Very Large Telescope (VLT). This is a cross-dispersed échelle spectrograph, which in the standard mode and the adopted configuration (1 arcsec slit width, red arm, and grating #520) yields a resolving power of 40 000. With exposure time of 3000 s, at an airmass of 1.35 and a seeing of about 0.9 arcsec, we obtained a S/N pixel⁻¹ at $\lambda \sim 5500$ Å of 210.

All reduction steps were performed within the UVES pipeline (version 5.2.0) and REFLEX². Neither binning nor smoothing was applied to the échelle spectrum. The spectrum, normalized by fitting a low order polynome to carefully selected continuum points, covers the wavelength range 4170–6200 Å, with a 60 Å wide gap at about 5200 Å.

To analyse the spectrum, we computed model atmospheres of Stock 16-12 using the LLMODELS stellar model atmosphere code (Shulyak et al. 2004). For all the calculations local thermodynamical equilibrium (LTE) and plane-parallel geometry were assumed. Convection was implemented according to the Canuto & Mazzitelli (1991, 1992) model of convection (see Heiter et al. 2002, for more details). We used the Vienna Atomic Line Database (VALD; Piskunov et al. 1995; Kupka et al. 1999; Ryabchikova et al. 1999) as a source of atomic line parameters for opacity calculations and abundance analysis.

We measured the radial velocity (v_r) and the projected rotational velocity ($v \sin i$) by fitting synthetic spectra, calculated with SYNTH3 (Kochukhov 2007), to the observed profiles of weakly blended lines, obtaining $v_r = -18.0 \pm 1.0$ km s⁻¹ and $v \sin i = 68.0 \pm 4.0$ km s⁻¹.

To determine the fundamental atmospheric parameters we used both hydrogen and metallic lines. To spectroscopically estimate the effective temperature (T_{eff}) and surface gravity ($\log g$) from hydrogen lines, we fitted synthetic line profiles to the observed H γ and H β lines. The adopted spectral synthesis code, SYNTH3, incorporates the algorithm by Barklem, Piskunov & O'Mara (2000)³ which takes into account not only self-broadening but also Stark broadening (see their section 3). The fit to the two covered hydrogen lines led to $T_{\text{eff}} = 8100 \pm 400$ K and $\log g = 4.0 \pm 0.4$ dex (see Fig. 2). The rather large error bars are due to uncertainties in the normalization and to the small, though not negligible, sensitivity of the hydrogen line wings to gravity variations.

The metallic-line spectrum provides further constraints on the atmospheric parameters. The presence of rather strong line blending, due to $v \sin i$ and to the overabundance of various elements, did not allow us to measure spectral lines with equivalent widths. We therefore analysed the metallic lines using synthetic spectra.

We first selected the least blended metallic lines with a well defined continuum level and then, for a given set of atmospheric parameters (T_{eff} , $\log g$, and microturbulence velocity – v_{mic}), fit the abundance of each selected line using the tools described in (Fossati et al. 2007, 2008). We repeated this operation for a set of atmospheric parameters ranging from 8000 to 9000 K in T_{eff} , from 3.6 to 4.5 dex in $\log g$, and from 2.0 to 5.0 km s⁻¹ in v_{mic} . We adopted steps of 100 K in T_{eff} , 0.1 dex in $\log g$, and 0.1 km s⁻¹ in v_{mic} . For each given set of atmospheric parameters and abundances we then calculated a synthetic spectrum covering the observed wavelength range. We finally determined the overall (excluding the regions covered by the hydrogen lines and the Na I D lines at $\lambda \sim 5892$ Å affected by strong non-LTE effects) best fitting synthetic spectrum, hence set of atmospheric parameters and abundances, using χ^2 statistics.

In the considered temperature regime and in particular for the spectral region bluewards of H β , the continuum level is extremely sensitive to temperature variations. This would lead to the introduction of a bias in the χ^2 minimization if applied using an observed spectrum with a fixed normalization, i.e. the χ^2 would be driven mostly by the fit to the continuum level, rather than by the fit to the metallic lines. To avoid this problem we renormalized the observed spectrum in order to perfectly match the continuum level of each calculated synthetic spectrum. In this way, variations of the χ^2 are due exclusively to the quality of the fit of the single spectral features. Using this technique we obtained $T_{\text{eff}} = 8700 \pm 200$ K, $\log g = 4.2 \pm 0.4$ dex, and $v_{\text{mic}} = 3.7 \pm 0.3$ km s⁻¹.

The two adopted parameter indicators did not lead to consistent effective temperature values. This could be due to various systematics affecting the determination of the atmospheric parameters (T_{eff} in particular) with the adopted indicators. In particular hydrogen lines recorded with échelle spectra are usually difficult to normalize. In this case, the normalization of the hydrogen lines was particularly uncertain due to the ‘wavy’ shape of the not-normalized reduced spectrum. In addition, Fossati et al. (2011) showed that a determination of the atmospheric parameters based on the abundance fit of metallic lines might lead to an overestimation of the effective temperature of up to a few hundreds of Kelvin. On the basis of these considerations we finally set the effective temperature at $T_{\text{eff}} = 8400 \pm 400$ K and the surface gravity at $\log g = 4.1 \pm 0.4$ dex. Having fixed T_{eff} and $\log g$ we then used the metallic lines and the method described above to determine the best-fitting v_{mic} , obtaining $v_{\text{mic}} = 3.4^{+0.7}_{-0.3}$ km s⁻¹.

The only way to solve the problem of the discordant effective temperature values would be to use further parameter indicators, such as photometry, which could be directly converted to fundamental parameters (T_{eff} and $\log g$) or calibrated to physical units to fit the spectral energy distribution (SED). Unfortunately, both methods are strongly affected by interstellar reddening, which for the Stock 16 open cluster is not known well enough to ensure an effective temperature determination more reliable than that provided by the hydrogen and metallic lines. Furthermore, a slight differential reddening in the young cluster results in a large uncertainty if using the mean reddening of the cluster.

We finally measured the abundance of 18 elements (see Table 1) obtaining an abundance pattern which well resembles that of CP metallic-line stars (Am stars). Fig. 3 shows the derived abundance pattern, relative to that of the Sun (Asplund et al. 2009), in comparison with the average abundance of the Am stars member of the Praesepe open cluster (Fossati et al. 2007, 2008) and of the Ap star HD 204411 which has an effective temperature similar to that of Stock 16-12 (Ryabchikova, Leone & Kochukhov 2005). The abundance pattern of Stock 16-12 presents all classical chemi-

² <http://www.eso.org/sci/software/reflex/>

³ <http://www.astro.uu.se/~barklem/hlinop.html>

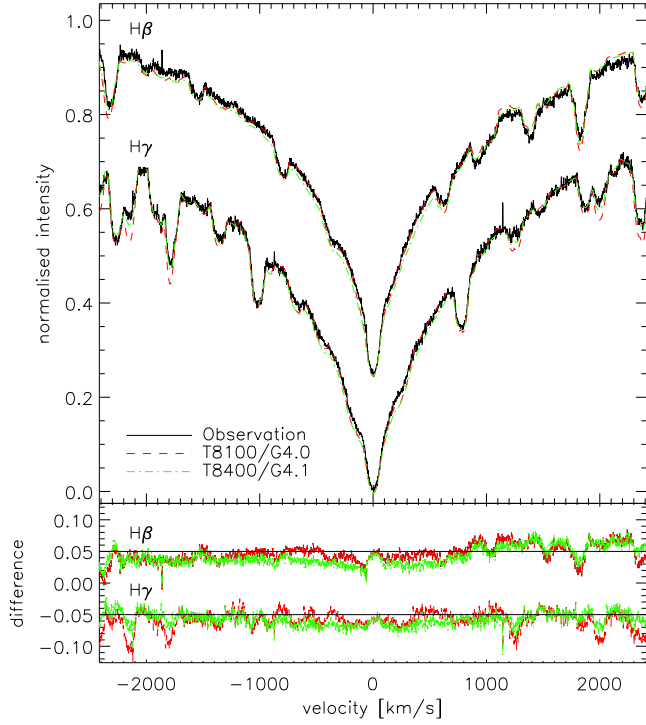


Figure 2. Top panel: comparison between the observed H γ and H β line profile (black solid line) and synthetic profiles calculated with the final adopted parameters (dash-dotted green line) and with the parameters which were found to best fit the hydrogen line profiles (dashed red line). The H γ line profile was rigidly shifted downwards by 0.2. The wavelength dimension has been converted in velocity and centred at the laboratory wavelength of the H β and H γ lines, respectively. Bottom panel: difference between the synthetic and observed H γ and H β line profiles rigidly shifted respectively downwards and upwards by 0.05. The line colours and styles are as for the top panel.

cal signatures of Am stars: underabundances of C, N, O, Ca⁴, and Sc, as well as overabundances of Fe-peak and rare-earth elements. Stock 16-12 shows also a slight overabundance of Na, which is not classically considered as a CP element in Am stars, though Fossati et al. (2007) found it to be systematically overabundant in each analysed Am star, and Takeda et al. (2012) found it to directly correlate with Fe in early F- and A-type stars. Note that we determined the sodium abundance using the lines at $\lambda \sim 5688 \text{ \AA}$ which are very little affected by non-LTE effects; we did not use the Na I D lines at $\lambda \sim 5892 \text{ \AA}$ which would instead lead to a strong Na overabundance due to non-LTE effects. The strong blending did not allow us to measure the abundance of other elements which are known to be overabundant in Am stars (i.e., V, Co, Cu, Zn, Zr, Pr, Sm, Gd, Dy, Ho, Er, and Yb). Nevertheless, the observed spectrum would still be well fitted when assuming an overabundance of 0.5 dex for V, Co, Cu, Zn, and Zr and of 1.5 dex for Pr, Sm, Gd, Dy, Ho, Er, and Yb, as expected for Am stars.

For stars in the temperature regime of Stock 16-12, variations on the effective temperature have the largest impact on abundance values (see e.g., Fossati et al. 2009). For this reason, and given the large difference in T_{eff} obtained using hydrogen and metal lines, it is important to check the abundance pattern still resembles that

Table 1. LTE atmospheric abundances of Stock 16-12 with the error estimates based on the internal scattering from the number of analysed lines, n . The third column gives the variation in abundance estimated by increasing T_{eff} by 400 K. The fifth column gives the abundances of Stock 16-12 relative to the solar values from Asplund et al. (2009). The last column lists the abundances of the solar atmosphere calculated by Asplund et al. (2009).

Ion	Stock 16-12				Sun $\log(N/N_{\text{tot}})$
	$\log(N/N_{\text{tot}})$	ΔT_{eff}	n	$[N_{\text{el}}/N_{\text{H}}]$	
C	-4.10	0.25	1	-0.49	-3.61
O	-3.52	0.03	1	-0.17	-3.35
Na	-5.58	0.36	1	+0.22	-5.80
Mg	-4.58	0.21	1	-0.14	-4.44
Si	-4.41	0.06	1	+0.12	-4.53
Ca	-5.90 \pm 0.05	0.32	3	-0.20	-5.70
Sc	-9.58	0.18	1	-0.69	-8.89
Ti	-6.85 \pm 0.26	0.05	2	+0.24	-7.09
Cr	-5.94 \pm 0.04	0.34	2	+0.46	-6.40
Mn	-6.14	0.38	1	+0.47	-6.61
Fe	-4.15 \pm 0.12	0.24	41	+0.39	-4.54
Ni	-5.33	0.34	1	+0.49	-5.82
Sr	-8.35	0.75	1	+0.27	-9.17
Y	-8.76 \pm 0.08	0.19	2	+1.07	-9.83
Ba	-8.43 \pm 0.23	0.46	2	+1.43	-9.86
La	-9.33 \pm 0.18	0.68	2	+1.61	-10.94
Ce	-9.12 \pm 0.04	0.59	3	+1.34	-10.46
Nd	-9.30 \pm 0.13	0.31	2	+1.32	-10.62
T_{eff}	8400 K				5777 K
$\log g$	4.1 dex				4.44 dex

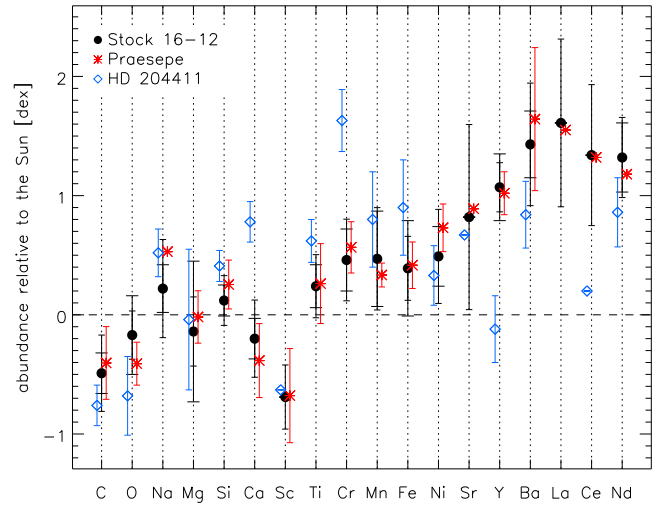


Figure 3. Element abundance relative to the Sun of the Stock 16-12 atmosphere (full black points) in comparison to the average abundance (red asterisks) of the Am stars member of the Praesepe open cluster (Fossati et al. 2007, 2008) and of the Ap star HD 204411 which has an effective temperature similar to that of Stock 16-12 (Ryabchikova, Leone & Kochukhov 2005). For all objects the same solar abundance set (Asplund et al. 2009) was used. Each abundance value of Stock 16-12 is shown with two uncertainty values: the standard deviation from the mean (column 2 of Table 1; assumed to be 0.2 dex for the elements analysed from just one line) and the uncertainty obtained by adding in quadrature the standard deviation from the mean and the variation in abundance due to an increase of 400 K in effective temperature (column 3 of Table 1).

⁴ Note that an underabundance of Ca is not necessarily present in Am CP stars.

of an Am star when accounting for the uncertainty on T_{eff} . The abundances of Stock 16-12 shown in Fig. 3 present two error bars, where the larger one takes into account also the uncertainty due to an increase in T_{eff} by 400 K. Even with the larger uncertainty the abundance pattern of Stock 16-12 resembles well that of Am stars, confirming therefore its classification.

The rather large v_{mic} value we derived from the UVES spectrum is in line with that typical of Am stars (Landstreet 1998; Landstreet et al. 2009). Nevertheless, the behaviour of the microturbulence velocity in very young (PMS) stars is not yet understood. Abundance analysis of young stars in the same temperature regime of Stock 16-12 shows an average v_{mic} value between 2.5 and 3 km s⁻¹ (Folsom et al. 2012; Zwintz et al. 2013), slightly enhanced compared to that of MS stars of the same temperature, though somewhat smaller than what we obtained for Stock 16-12. This further strengthens the conclusion that Stock 16-12 is a CP Am star.

However, CP Am stars are commonly found in close binary systems (Abt & Levy 1985; Debernardi et al. 2000). To check whether Stock 16-12 is member of a close binary, we derived the star's radial velocity from an interrupted UVES exposure, obtained within the same service mode observing programme on 2013 April 28 (exposure time 722 s; S/N pixel⁻¹ at $\lambda \sim 5500 \text{ \AA}$ of 49), and two further UVES spectra obtained within a Director's Discretionary Time (DDT) programme on 2014 April 12 with exposure times of 1205 s and a S/N of 56 and 52, respectively. Using the same method as applied on the high S/N spectrum, we measured a consistent radial velocity of $v_r = -18.0 \pm 1.0 \text{ km s}^{-1}$. Thus, we conclude that Stock 16-12 is probably not in a binary system, unless it is a wide binary with a period of several years.

To gather more information on the CP nature of the star, we obtained Focal Reducer and Low Dispersion Spectrograph 2 (FOR2) spectropolarimetric observations to attempt the detection of a large scale magnetic field. The FOR2 low-resolution spectropolarimeter (Appenzeller & Rupprecht 1992; Appenzeller et al. 1998) is attached to the Cassegrain focus of the 8-m Antu telescope of the ESO VLT of the Paranal Observatory. The observations were performed using the 2k × 4k MIT CCDs (pixel size 15 $\mu\text{m} \times 15 \mu\text{m}$) and a slit width of 1.0 arcsec in order to collect more photons and increase the S/N. We also adopted the 200 kHz/low/1 × 1 read-out mode and the GRISM 1200B. Each spectrum covers the 3700–5100 \AA spectral range which includes most of the Balmer lines, except H α , and a number of metallic lines. The star was observed once on 2014 April 18 with a sequence of spectra obtained rotating the quarter waveplate as follows: -45° , $+45^\circ$, $+45^\circ$, -45° . Each of the four spectra was obtained with an exposure time of 1568 s which led to a Stokes I spectrum with a S/N pixel⁻¹ calculated at 4950 \AA of about 1120. We reduced and analysed the FOR2 data using the routines and technique described in Bagnulo et al. (2012) and references therein, without detecting a magnetic field: by using the whole spectrum we obtained an average longitudinal magnetic field value $\langle B_z \rangle$ of $-11 \pm 76 \text{ G}$, while using the hydrogen lines we obtained $\langle B_z \rangle = -193 \pm 129 \text{ G}$. Hence, there is no evidence for a magnetic field with a strength typical of that of Ap stars.

4 CLUSTER MEMBERSHIP AND EVOLUTIONARY STATUS

Three previous studies list the object analysed here as member of Stock 16 (Fenkart et al. 1977; Turner 1985; Paunzen et al. 2005b), whereas Vázquez et al. (2005) denoted the star as probable non-

member by means of CCD $UBVR_I$ photometry. This last classification is probably due to the deviation from the cluster sequence in the $(U - B)/V$ CMD, since in all other colours no disagreement is noticeable. However, compared to the photoelectric $(U - B)$ measurement by Turner (1985), the CCD study provided a much redder colour by 0.14 mag. This can be attributed to well known difficulties in reproducing the standard $(U - B)$ colour with CCDs (see e.g., Sung & Bessell 2000). We therefore adopt the photoelectric measurement for this colour. The remaining colours in common between the investigations are in excellent agreement, also if compared with measurements by the AAVSO Photometric All-Sky Survey [APASS,⁵ Data Release 7 (DR7)], which provides data in the $B V g' r' i'$ filters.

Since the cluster is located at a distance of $\sim 1.9 \text{ kpc}$, proper motion as membership criterion is in general not that efficient anymore compared to nearby open clusters. Nevertheless, the average cluster motion given by Zejda et al. (2012) is in agreement with that listed in the UCAC4 (Zacharias et al. 2013) and PPMXL (Röser, Demleitner & Schilbach 2010) catalogues: $-5.7/3.0 (\pm 2.7)$ and $-5.7/5.5 (\pm 9.8) \text{ mas yr}^{-1}$, respectively. The errors for both directions are given in parentheses. By employing the method described by Balaguer-Núñez, Tian & Zhao (1998), which takes into account the individual errors, we derived kinematic membership probabilities for Stock 16-12 of 62 and 91 per cent using UCAC4 and PPMXL data, respectively.

The interstellar reddening is a further useful information to constrain membership. With the adopted spectroscopic stellar parameters and their uncertainties from Section 3, the empirical colour-temperature relation by Worthey & Lee (2011), and the observed colours, we determined $E(B - V) = 0.36 \pm 0.05 \text{ mag}$. The various colour excess ratios are well in line with a standard reddening law $R_V = 3.1$, which was also found by Vázquez et al. (2005) for the whole cluster. As comparison, we applied the Q -method (e.g., Gutierrez-Moreno 1975) to the photoelectric UBV data by Turner (1985) using stars in Stock 16 brighter than $V=13 \text{ mag}$, which are most likely earlier than spectral type A0 and reached already the MS. On the basis of 14 stars, we obtained a reddening range of $0.40 < E(B - V) < 0.56 \text{ mag}$. Hence, within the errors, the object lies on or slightly below the lower reddening border. On the other hand, the analysis by Kaltcheva, Golev & Moran (2014) of the surrounding Cen OB1 association shows that the bulk of foreground objects exhibits a reddening lower than the one of Stock 16-12. A detailed investigation of the cluster area with Strömgren photometry would be helpful to further constrain both reddening and membership.

Unfortunately, the derived radial velocity for the target star ($v_r = -18.0 \pm 1.0 \text{ km s}^{-1}$, see Section 3) does not provide an additional membership indication. Kharchenko et al. (2007) list an average velocity of $-42 \pm 9 \text{ km s}^{-1}$ using literature data for five O- and early B-type stars in the range of -21 to -74 km s^{-1} . However, according to Sana et al. (2012) more than 70 per cent of massive stars are part of binary systems. Indeed, most of these five objects are mentioned in the literature as radial velocity variables (e.g. by Crampton 1972). Nevertheless, the derived radial velocity is in very good agreement with the average value of the Cen OB1 association ($v_r = -20.0 \text{ km s}^{-1}$; Corti & Orellana 2013). Furthermore, the NaD lines in the spectrum show massive interstellar absorption lines, which would agree with the membership of the star in a young cluster or association, which still holds part of the original

⁵ <http://www.aavso.org/apass>

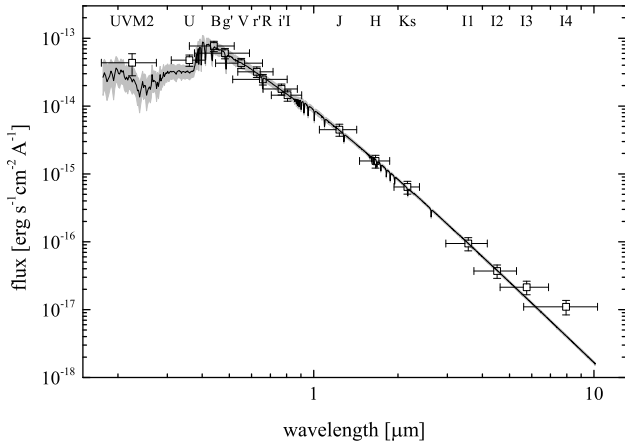


Figure 4. The SED of Stock 16-12 using the available photometric measurements in the UVOT, Johnson, SDSS, 2MASS, and IRAC bands (squares) compared to theoretical fluxes of the adopted model atmosphere (8400 K, black line). The grey area represents the differences to models with temperatures ± 400 K to indicate the changes in the flux. Furthermore, the width of the filters and the errors of the observed fluxes are given.

molecular cloud. In a few years the precise *Gaia* data will allow one to obtain an unambiguous membership determination.

The available optical, Two Micron All Sky Survey (2MASS; Skrutskie et al. 2006), and Galactic Legacy Infrared Mid-Plane Survey Extraordinaire (GLIMPSE) Infrared Array Camera (IRAC) data (Churchwell et al. 2009) already allow one to construct a SED from 0.36 to $8\mu\text{m}$ (see Fig. 4). To extend the SED more to the ultraviolet range, we have analysed an observation in the *UVM2* band ($\sim 2200\text{Å}$) of the UV/Optical Telescope (UVOT; Poole et al. 2008) on board of the *Swift* satellite. We have applied aperture photometry with the UVOT specific tasks in the HEASOFT package (version 6.15) and obtained 17.60 ± 0.05 mag (AB).

All data were dereddened using the derived $E(B - V)$, $R_V = 3.1$, and the extinction curve model by Fitzpatrick (1999). The excellent agreement with the model atmosphere confirms the adopted reddening and thus the spectroscopic temperature. To fit the fluxes of the derived stellar atmosphere from Section 3 to the photometry, one of the coupled parameters (distance and stellar radius) has to be fixed. Owing to the large uncertainties in the stellar parameters, especially in $\log g$, Stock 16-12 can cover radii between ~ 1.5 – $4 R_\odot$ according to evolutionary models by Lagarde et al. (2012) [using the zero-age main sequence (ZAMS) as upper limit for gravity]. With these extrema we obtain distances from the SED of 1.0 and 2.8 kpc, respectively. In contrast, the mean cluster distance of 1.9 kpc requires a radius of $\sim 2.75 R_\odot$ for a proper fit.

What can be immediately recognized in Fig. 4 is the noticeable IR-excess, starting at $5.8\mu\text{m}$. The IRAC band at $8\mu\text{m}$ deviates already more than 1 mag from the theoretical flux. This corresponds to more than three times of the total error budget, calculated using the error propagation by Fitzpatrick (1999) including $\sigma_{R_V} = 0.2$ and the individual photometric errors. This is an indication for the presence of circumstellar material around a young (PMS) object. Therefore, a connection with the young environment is most likely. On the other side of the covered wavelength range one can also notice emission in the near-UV, which is in general a sign of accretion. However, the position of the UVOT *UVM2* filter coincides with the UV bump at 2175Å of extinction curve models (see e.g. Fitzpatrick 1999). It is therefore strongly affected by systematic uncertainties

in the extinction law. Furthermore, the strength, position, and width of the UV bump depend on the line of sight. Although UV spectra are preferable, also observations in the additional UVOT bands (*UVW1* and *UVW2*) could provide hints about its strength and the real nature of the possible UV excess. The deviation observed at UV wavelengths could be also explained by an underestimation of the effective temperature or an overestimation of the interstellar reddening. Note however that a decreased reddening would lead to a worse fit of the other available photometry and that the excess in the UV is still present when using a higher effective temperature, i.e. 8800 K.

We also applied the SED fitting tool by Robitaille et al. (2007), which was especially built to deal with young stellar objects and allows to fit all parameters simultaneously⁶. By permitting extreme ranges for the distance ($d \leq 5$ kpc) and extinction ($A_V \leq 5$ mag), the best model fit was achieved with a total $\chi^2 = 21$ (14 degrees of freedom), resulting in the parameters $A_V = 1.23$ (including 0.1 mag circumstellar extinction), $d = 2.4$ kpc, $T_{\text{eff}} = 8976$ K, and $R = 3.3 R_\odot$ (their model ID 3017872). The extinction value is close to the one adopted above, the distance is in reasonable agreement to that reported for Stock 16, and the temperature only slightly above the spectroscopic range ($T_{\text{eff}} = 8400 \pm 400$ K). The latter can be explained by the somewhat higher reddening and to some extent also by the use of solar metallicity models in the fitting tool.

In consideration of all available information we therefore conclude that a foreground position of the target star can be excluded and a membership to Stock 16 or the young association is instead very likely. This is also justified by the reasonable agreement of the positions in the Hertzsprung-Russell diagram (HRD) using the cluster distance and the purely spectroscopic results (Fig. 5). We would like to point out that a correction of the object's brightness by 0.75 mag (binarity with mass ratio $q = 1$) results in an exceptional good coincidence with the spectroscopic luminosity value (indicated by the cross in Fig. 5). However, a binary nature is unlikely as discussed in Section 3. Nevertheless, the position above the ZAMS supports the PMS nature inferred from the IR-excess, especially if considering the more precise cluster distance. The interpolation within the PMS evolutionary tracks by Lagarde et al. (2012) results in $2.3 \pm 0.2 M_\odot$ and an age of 4 ± 1 Myr for the 'photometric' position in the HRD, whereas the purely spectroscopic one indicates $1.95 M_\odot$ and 6 Myr. In the last case, the uncertainty especially in age is very large, reaching ~ 15 Myr towards the ZAMS. The derived ages are well in line with the age of Stock 16 listed in the literature (3–8 Myr).

5 DISCUSSION

In the previous sections we have shown that Stock 16-12 is an intermediate-mass PMS star, which already shows all abundance characteristics of a CP Am star.

The estimated stellar age of 4–6 Myr is of extreme importance because it allows one to put an observational upper limit on the time-scale of diffusion processes. To our knowledge, the only work which presented stellar models with atomic diffusion for PMS stars is Vick et al. (2011). The earliest appearance of noticeable surface abundance anomalies strongly depends on the mass, whereas low mass loss rates influence the amplitude of peculiarities. Previous

⁶ Note that the UVOT filters are currently not included.

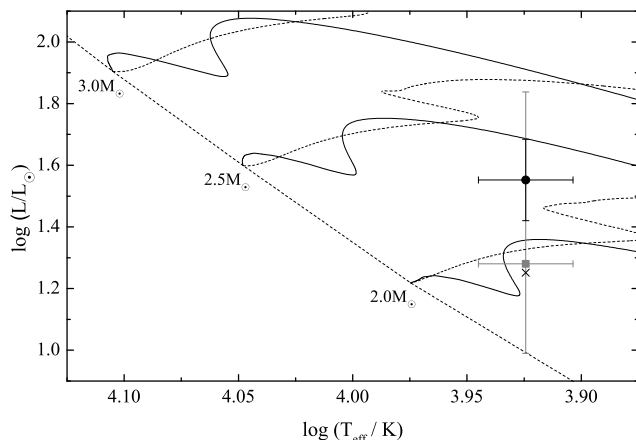


Figure 5. The position of Stock 16-12 in the HRD using the V-band magnitude, cluster distance and spectroscopic temperature (black circle and error bars), and corrected for binarity with $q = 1$ (cross). Furthermore, the purely spectroscopic results were transformed to the temperature/luminosity plane (grey square and error bars). The PMS tracks for solar metallicity with standard prescriptions by Lagarde et al. (2012) are indicated as solid lines, whereas ZAMS, MS, and post MS tracks are given as comparison by dashed lines.

calculations, able to reproduce the observed abundances, have already shown that low mass-loss rates ($< 10^{-13} M_{\odot} \text{ yr}^{-1}$) for Am stars are likely (Michaud et al. 1983; Vick et al. 2011).

The evolution of Ca abundance presented by Vick et al. (2011) is probably of particular interest, since this element shows a strong variation with age. As can be recognized in their fig. 1, the higher mass models ($\geq 1.9 M_{\odot}$) predict a short duration ($< 1 \text{ Myr}$) of underabundance, followed by an abrupt change to even significant overabundances. The underabundance dips are located at about 3.5 and 6.5 Myr for the 2.5 and 1.9 M_{\odot} models, respectively. These ages are well in line with our results for the mass, age, and the derived Ca underabundance for Stock 16-12. However, there is a strong temperature dependency (see Table 1) for this element, resulting in even slight overabundances at the adopted upper age limit. Nevertheless, also the evolution of other presented elements (e.g. O, Mn, or Ni) is in agreement with the age and abundance pattern of Stock 16-12.

Probably the least agreement can be found for Fe, which needs, according to the lower mass models, too long to show the measured overabundance of $\sim 0.4 \text{ dex}$, but the 2.5 M_{\odot} model shows a small peak ($\sim 0.15 \text{ dex}$) at the same age as Ca discussed above. The Fe abundance at the lower border of the adopted temperature range would also be in reasonable agreement to the model. Also the higher abundance for this element might be reproduced, though with a much lower mass loss rate than $5 \times 10^{-14} M_{\odot} \text{ yr}^{-1}$ used by Vick et al. (2011). However, also a slightly higher initial metallicity of the host cluster (and thus also of the star) can be responsible.

Chemical peculiarities in Am stars seem to depend also on the stellar rotational velocity (Fossati et al. 2008), but it is unsure whether this holds also for PMS stars. Nevertheless, it is worth to obtain a hint of the expected rotational velocity at the ZAMS. Based upon the PMS models by Haemmerlé et al. (2013), which include the rotational evolution, the equatorial velocity of the object will be increased by about 30 per cent, though their comparison of the models with the measured rotation rates of Herbig Ae/Be objects shows only a poor agreement. Assuming that the measured

$v \sin i$ represents roughly the true rotational velocity, the target star would reach a velocity of about 90 km s^{-1} at the ZAMS, which is close to the upper end of the velocity distribution of Am stars (Abt & Morrell 1995).

The possible UV excess (see discussion in Section 4), which could be interpreted as accretion, has also natural consequences on the elemental distribution in the stellar atmosphere. If further observations indicate that accretion is still in process, the rate has to be smaller than $10^{-14} M_{\odot} \text{ yr}^{-1}$ to have no influence on the chemical separation (Vick et al. 2011).

Our non-detection of a magnetic field does not rule completely out the presence of a magnetic field, since the star might have been observed at an unlucky phase. Therefore, one cannot exclude that the star is magnetic and that the current Am abundance pattern of Stock 16-12 might change before the star reaches the ZAMS in order to match that of magnetic CP stars. So far, V380 OriA is the only candidate which shows weak Ap/Bp peculiarities (Folsom et al. 2012) and a magnetic field. Since the star is about twice as massive as Stock 16-12, its evolution is much faster too. Additional spectropolarimetric observations for Stock 16-12 and the detection of more CP PMS stars would be essential to test this hypothesis.

6 CONCLUSION

We presented here a detailed parameter determination and abundance analysis for the star Stock 16-12. From the spectroscopic data we determined a temperature of $8400 \pm 400 \text{ K}$, a surface gravity of $\log g = 4.1 \pm 0.4 \text{ dex}$, and a microturbulence velocity of $v_{\text{mic}} = 3.4^{+0.7}_{-0.3} \text{ km s}^{-1}$. Additional spectroscopic data allowed us to conclude that the object is probably a single star. Furthermore, we have not detected a magnetic field using spectropolarimetric observations obtained at one epoch.

The star's abundance pattern resembles well that of CP metallic-line (Am) stars. All currently available data suggest that the star is a member of the very young (3–8 Myr) open cluster Stock 16, or at least to belong to the young Cen OB1 association in which the cluster is embedded. Depending on the adoption of either the purely spectroscopic results or the cluster distance, we determined a stellar mass range of about $1.95\text{--}2.3 M_{\odot}$. The membership to a very young region, the noticeable IR-excess, and the stellar age of 4–6 Myr inferred from evolutionary models allow us to conclude that the object is still in its PMS stage. This star is probably the second PMS CP object known so far, and the very first showing typical Am star elemental abundances.

Young CP stars are extremely important to test and constrain the theory of atomic diffusion. Current available stellar evolutionary models are well in line with our results for the stellar mass, age, and the derived elemental abundances. However, the further evolution of Stock 16-12 is unclear, in particular if the star hosts a structured magnetic field. In this case, the star might develop its current Am abundance pattern into that of MS magnetic CP stars before it reaches the ZAMS. Additional spectropolarimetric measurements and the detection of more CP PMS stars are needed to test this hypothesis.

ACKNOWLEDGEMENTS

Based on observations made with ESO telescopes at the La Silla Paranal Observatory under programme ID 091.C-0498 and 292.C-

5044. This research has made use of data, software, and/or web tools obtained from NASA's High Energy Astrophysics Science Archive Research Center (HEASARC), a service of Goddard Space Flight Center and the Smithsonian Astrophysical Observatory. This research was also made possible through the use of the AAVSO Photometric All-Sky Survey (APASS), funded by the Robert Martin Ayers Sciences Fund. Furthermore, we made use of the SIMBAD data base and VizieR catalogue access tool, CDS, Strasbourg, France, and the WEBDA data base, operated at the Department of Theoretical Physics and Astrophysics of the Masaryk University. MN acknowledges the support by the grant 14-26115P of the Czech Science Foundation. KZ acknowledges support from the Fund for Scientific Research of Flanders (FWO), Belgium, under grant agreement G.0B69.13. EP is financed by the SoMoPro II programme (3SGA5916). The research leading to these results has acquired a financial grant from the People Programme (Marie Curie action) of the Seventh Framework Programme of EU according to the REA Grant Agreement No. 291782. The research is further co-financed by the South-Moravian Region. It was also supported by the grant 7AMB14AT015, and the financial contributions of the Austrian Agency for International Cooperation in Education and Research (BG-03/2013 and CZ-09/2014). This work reflects only the author's views and the European Union is not liable for any use that may be made of the information contained therein.

REFERENCES

- Abt H. A., Levy S. G., 1985, *ApJS*, 59, 229
 Abt H. A., Morrell N. I., 1995, *ApJS*, 99, 135
 Appenzeller I., Rupprecht G., 1992, *Messenger*, 67, 18
 Appenzeller I. et al., 1998, *Messenger*, 94, 1
 Asplund M., Grevesse N., Sauval A. J., Scott P., 2009, *ARA&A*, 47, 481
 Bagnulo S., Landstreet J. D., Fossati L., Kochukhov O., 2012, *A&A*, 538, A129
 Bailey J. D., Landstreet J. D., Bagnulo S., 2014, *A&A*, 561, A147
 Balaguer-Núñez L., Tian K. P., Zhao J. L., 1998, *A&AS*, 133, 387
 Barklem P. S., Piskunov N., O'Mara B. J., 2000, *A&A*, 363, 1091
 Bressan A., Marigo P., Girardi L., Salasnich B., Dal Cero C., Rubele S., Nanni A., 2012, *MNRAS*, 427, 127
 Canuto V. M., Mazzitelli I., 1991, *ApJ*, 370, 295
 Canuto V. M., Mazzitelli I., 1992, *ApJ*, 389, 724
 Churchwell E. et al. 2009, *PASP*, 121, 213
 Corti M. A., Orellana R. B., 2013, *A&A*, 553, A108
 Crampton D., 1972, *MNRAS*, 158, 85
 Debernardi Y., Mermilliod J.-C., Carquillat J.-M., Ginestet N., 2000, *A&A*, 354, 881
 Fenkart R. P., Binggeli B., Good D., Jenni D., Labhardt L., Tschumi A., 1977, *A&AS*, 30, 307
 Fitzpatrick E. L., 1999, *PASP*, 111, 63
 Folsom C. P., Bagnulo S., Wade G. A., Alecian E., Landstreet J. D., Marsden S. C., Waite I. A., 2012, *MNRAS*, 422, 2072
 Fossati L., Bagnulo S., Landstreet J., Wade G., Kochukhov O., Monier R., Weiss W., Gebran M., 2008, *A&A*, 483, 891
 Fossati L., Bagnulo S., Monier R., Khan S. A., Kochukhov O., Landstreet J., Wade G., Weiss W., 2007, *A&A*, 476, 911
 Fossati L., Ryabchikova T., Bagnulo S., Alecian E., Grunhut J., Kochukhov O., Wade G., 2009, *A&A*, 503, 945
 Fossati L., Ryabchikova T., Shulyak D. V., Haswell C. A., Elmasli A., Pandey C. P., Barnes T. G., Zwintz K., 2011, *MNRAS*, 417, 495
 Gutierrez-Moreno A., 1975, *PASP*, 87, 805
 Haemmerlé L., Eggenberger P., Meynet G., Maeder A., Charbonnel C., 2013, *A&A*, 557, A112
 Heiter U. et al., 2002, *A&A*, 392, 619
 Jaschek M., Jaschek C., 1974, *Vistas Astron.*, 16, 131
 Kaltcheva N. T., Georgiev L. N., 1994, *MNRAS*, 269, 289
 Kaltcheva N., Golev V., Moran K., 2014, *A&A*, 562, A69
 Kharchenko N. V., Scholz R.-D., Piskunov A. E., Röser S., Schilbach E., 2007, *Astron. Nachr.*, 328, 889
 Kochukhov O. P., 2007, in Romanyuk I. I., Kudryavtsev D. O., Neizvestnaya O. M., Shapoval V. M., eds, *Proc. Int. Conf., Physics of Magnetic Stars. Special Astrophysical Observatory, Nizhnij Arkhyz, Russia*, p. 109
 Kupka F., Piskunov N., Ryabchikova T. A., Stempels H. C., Weiss W. W., 1999, *A&AS*, 138, 119
 Lagarde N., Decressin T., Charbonnel C., Eggenberger P., Ekström S., Palacios A., 2012, *A&A*, 543, A108
 Landstreet J. D., 1998, *A&A*, 338, 1041
 Landstreet J. D., Kupka F., Ford H. A., Officer T., Sigut T. A. A., Silaj J., Strasser S., Townshend A., 2009, *A&A*, 503, 973
 Mermilliod J.-C., Paunzen E., 2003, *A&A*, 410, 511
 Michaud G., Tarasick D., Charland Y., Pelletier C., 1983, *ApJ*, 269, 239
 Paunzen E., Stütz Ch., Maitzen H. M., 2005a, *A&A*, 441, 631
 Paunzen E., Netopil M., Iliev I. K., Maitzen H. M., Claret A., Pintado O. I., 2005b, *A&A*, 443, 157
 Paunzen E., Netopil M., Pintado O. I., Rode-Paunzen M., 2011, *Astron. Nachr.*, 332, 77
 Piskunov N. E., Kupka F., Ryabchikova T. A., Weiss W. W., Jeffery C. S., 1995, *A&AS*, 112, 525
 Poole T. S. et al. 2008, *MNRAS*, 383, 627
 Preston G. W., 1974, *ARA&A*, 12, 257
 Richer J., Michaud G., Turcotte S., 2000, *ApJ*, 529, 338
 Robitaille T. P., Whitney B. A., Indebetouw R., Wood K., 2007, *ApJS*, 169, 328
 Röser S., Demleitner M., Schilbach E., 2010, *AJ*, 139, 2440
 Ryabchikova T. A., Piskunov N. E., Stempels H. C., Kupka F., Weiss W. W., 1999, *Phys. Scr.*, T83, 162
 Ryabchikova T., Leone F., Kochukhov O., 2005, *A&A*, 438, 973
 Sana H. et al., 2012, *Science*, 337, 444
 Santos-Silva T., Gregorio-Hetem J., 2012, *A&A*, 547, A107
 Shulyak D., Tsybal V., Ryabchikova T., Stütz Ch., Weiss W. W., 2004, *A&A*, 428, 993
 Skrutskie M. F. et al., 2006, *AJ*, 131, 1163
 Sung H., Bessell M. S., 2000, *Publ. Astron. Soc. Aust.*, 17, 244
 Takeda Y., Kang D.-I., Han I., Lee B.-C., Kim K.-M., Kawanomoto S., Ohishi N., 2012, *PASJ*, 64, 38
 Titus J., Morgan W. W., 1940, *ApJ*, 92, 256
 Turner D. G., 1985, *ApJ*, 292, 148
 Vázquez R. A., Baume G. L., Feinstein C., Nuñez J. A., Vergne M. M., 2005, *A&A*, 430, 471
 Vick M., Michaud G., Richer J., Richard O., 2011, *A&A*, 526, A37
 Watson W. D., 1971, *A&A*, 13, 263
 Worthey G., Lee H.-C., 2011, *ApJS*, 193, 1
 Zacharias N., Finch C. T., Girard T. M., Henden A., Bartlett J. L., Monet D. G., Zacharias M. I., 2013, *AJ*, 145, 44
 Zejda M., Paunzen E., Baumann B., Mikulášek Z., Liška J., 2012, *A&A*, 548, A97
 Zwintz K. et al., 2013, *A&A*, 552, A68